Proceedings of the 12th International Conference on Fluid Flow, Heat and Mass Transfer (FFHMT 2025)
July 15, 2025 - July 17, 2025 | Imperial College London Conference, London, United Kingdom
Paper No. 153
DOI: 10.11159/ffhmt25.153

Determining the Diffusion Coefficient for Articular Cartilage Modelled As Homogeneous and Porous Material

Anna Skorupa[1], Alicja Piasecka-Belkhayat[1]
[1]Department of Computational Mechanics and Engineering, Silesian University of Technology
Konarskiego 18A, 44-100 Gliwice, Poland
anna.skorupa@polsl.pl, alicja.piasecka-belkhayat@polsl.pl

Abstract - Porous materials are defined as materials consisting of a 'matrix' in which the voids are filled with gas or liquid. Porous materials also include biological tissues, because they consist of dispersed cells isolated by voids (pores) through which nutrients flow to all cells in them. An example of such tissue is articular cartilage, in which the size of the pores is estimated to be between 2 nm and 6 nm. The study involved determining the diffusion coefficient value for a selected tissue (articular cartilage) during cooling, assuming a model for homogeneous and porous material. The results obtained confirm that the applied material model impacts on the values of the diffusion coefficient. Higher coefficient values were obtained for the model taking into account the porosity of the sample than for the homogeneous material model. In addition, a decrease in temperature causes a decrease in the diffusion coefficient value. The results obtained can be used in the future to analyse the behaviour of a biological sample during the cryopreservation process.

***Keywords*:** diffusion coefficient, porous media, heat transfer, mass transfer, articular cartilage

1. Introduction

Porous materials are defined as materials consisting of a 'matrix' in which the pores are filled with fluid. Their characteristic feature is the porosity, which defines the ratio of the volume of the pores to the volume of the entire material. Due to the application of porous materials in many fields, the transport phenomena occurring in them are carried out more often, for example, analyses of electronic devices or thermal insulation in buildings, as well as porous scaffolds for tissue engineering and transport in biological tissues [1], [2].

Biological tissues consist of dispersed cells isolated by voids (pores) through which nutrients flow to all cells in them. Therefore, they can be considered as porous materials. Transport phenomena that can occur in biological tissues include, for example, heat and mass transfer. Heat transfer in biological tissues is related to processes such as heat conduction in tissues or heat transfer by perfusion of blood through tissue pores (blood convection). Mass transport in tissues is induced by the phenomenon of diffusion. Assuming that tissues are porous materials, mass transfer is mainly explored in the context of drug and nutrient transport, e.g. to brain cells, or the transport of elements that are part of biodegradable scaffolds [2].

Biological tissue, such as articular cartilage, is often modelled as a homogeneous material [3]–[6]. However, this is a simplification, as articular cartilage represents an example of a porous material. Articular cartilage is a thin connective fibrocartilage composed of water (approximately 80%), collagens, and proteoglycans. The size of the pores present in the tissue is estimated to be in the range of 2 nm to 6 nm [7]–[9]. Therefore, it is reasonable to examine the influence of the porous material properties on the diffusion coefficient, which is a crucial parameter for correctly simulating the changes in cryoprotectant concentration in a biological sample.

This article presents a comparison of the diffusion coefficient values calculated for biological tissue treated as homogeneous material and as a porous medium. For the homogeneous material, the effective diffusion coefficient is determined using the Einstein-Stokes equation. When the material was assumed to be porous, a modified relationship was applied, considering the porosity and tortuosity of the biological tissue. In the mathematical model, the diffusion coefficient also depends on the temperature distribution in the tissue. The analysis was performed for a selected biological tissue (articular cartilage) to simulate changes during its temperature reduction process.

2. Methodology

In this study, a biological tissue sample (articular cartilage) was modelled and a two-dimensional axisymmetric domain was analysed [3]–[6]. A simplified scheme of the computational domain (Ω) is depicted in Fig. 1. The variable temperature distribution in the tissue is the result of changes in the temperature of the bath solution, which was reduced at a cooling rate of 100 °C·min^{-1}. This is the cooling rate that is used during cryopreservation by method called vitrification [10], [11]. It is assumed that bath solution consists of water and dimethylsulphoxide (DMSO) with the concentration equal to c_{bath} = 10 %(w/w).

In the following subsections, a mathematical and numerical model of the problem is presented.

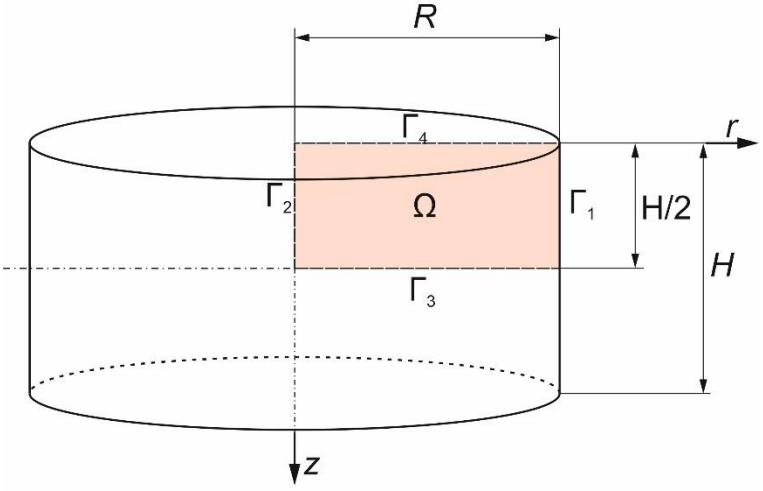

Fig. 1: Domain considered, where R and H are dimensions, $\Gamma_{1\text{-}4}$ are the boundaries of the domain.

2.1. Mathematical model

To determine the effective diffusion coefficient D_{eff} in homogeneous materials the Einstein-Stokes equation is used [5], [12]:

$$D_{eff}(T) = \frac{k_B T}{6\pi r_s \mu_d}, \tag{1}$$

where k_B is the Boltzmann constant (k_B = 1.38×10^{-23} J·K^{-1}), T is the temperature (in [K]), r_s is the radius of the spherical particle and μ_d is dynamic viscosity of DMSO.

For porous media, the diffusion coefficient is modified to take into account the porosity and tortuosity of the material. The effective diffusion coefficient (D_{eff}) is expressed as [13]–[15]:

$$D_{eff} = D_{dw}\frac{\varepsilon}{\tau^2}, \tag{2}$$

where D_{dw} is the diffusion coefficient of DMSO in water, ε is the water content in the sample and τ is the tortuosity factor. The diffusion coefficient of DMSO in water can be calculated as follows [13], [15]:

$$D_{dw} = D_0 + \Gamma^{0.5}, \tag{3}$$

where D_0 is the reference diffusion coefficient, Γ is the thermodynamic factor of the form [13], [15]:

$$\Gamma = 1 + x_d\left(\frac{\partial ln\gamma_d}{\partial x_d}\right), \tag{4}$$

where x_d is the mole fraction of DMSO and γ_d is the activity coefficient for DMSO, which is calculated using the UNIFAC model [16].

The reference diffusion coefficient can be expressed [13], [15]:

$$D_0 = \left(D_{0,dw}\right)^{x_w} + \left(D_{0,wd}\right)^{x_d}, \tag{5}$$

where $D_{0,dw}$ and $D_{0,dw}$ are the diffusion coefficients at infinite-dilution of DMSO in water and water in DMSO, respectively. The diffusion coefficients are estimated by using the formulas proposed in [13], [15]:

$$D_{0,dw} = (2.98 \times 10^{-7})\mu_w \cdot \left(0.285V_{c,d}^{1,048}\right)^{-0.5473} \cdot T, \tag{6}$$

$$D_{0,dw} = (9.89 \times 10^{-8})\mu_d \cdot \left(0.285V_{c,d}^{1,048}\right)^{-0.45} \cdot \left(0.285V_{c,w}^{1,048}\right)^{0.265} \cdot T, \tag{7}$$

where μ_w is the dynamic viscosity of water, $V_{c,d}$ and $V_{c,w}$ are the critical volume of DMSO and water, respectively.

The unsteady temperature distribution in the selected biological tissue, on which the diffusion coefficient depends, is determined from the Fourier equation [5]:

$$c_p\rho\frac{\partial T(r,z,t)}{\partial t} = \nabla(k\nabla T), \tag{8}$$

where c_p is the specific heat capacity, ρ is the density, k is the thermal conductivity, r and z are the geometric coordinates of the cylindrical coordinate system, t is the time and ∇ is the gradient operator.

The unsteady heat transfer problem is supplemented with the initial condition $T(r, z, t = 0) = T_{int.}$ and boundary conditions [5]:

$$\begin{cases} \Gamma_1 \text{ and } \Gamma_4: & -\mathbf{n}k \cdot \nabla T = \alpha[T(r,z,t) - T_{bath}], \\ \Gamma_2 \text{ and } \Gamma_3: & -\mathbf{n}k \cdot \nabla T = 0, \end{cases} \tag{9}$$

where α is the natural convection heat transfer coefficient.

To calculate the mole fraction of DMSO, the mass transfer in the sample also needs to be determined [5]:

$$\frac{\partial c_d(r,z,t)}{\partial t} = \nabla\left(D_{eff}\nabla c_d\right), \tag{10}$$

where c_d is the concentration of DMSO in the sample.

The mass transfer model is completed by the initial condition c_d $(r, z, t = 0) = c_{int.}$ and boundary conditions [5]:

$$\begin{cases} \Gamma_1 \text{ and } \Gamma_4: & -\mathbf{n}D_{eff} \cdot \nabla c_d = 0.9c_{bath}, \\ \Gamma_2 \text{ and } \Gamma_3: & -\mathbf{n}D_{eff} \cdot \nabla c_d = 0. \end{cases} \tag{11}$$

2.2. Numerical model

The unsteady state heat transfer analysis is performed using the finite difference method (FDM) [5], [17]. A constant time grid is implemented:

$$t^0 < t^1 < \cdots < t^{f-1} < t^f < t^{f+1} < \cdots < t^\infty, \tag{12}$$

where $\Delta t = t^f - t^{f-1}$ is the time step.

A geometric grid was also introduced into the computational domain of the sample. The grid cell consists of five points – a central node and four nodes in four axial directions from the central node. Moreover, the boundary nodes are located half a mesh step away from the boundary of the domain.

According to the concept of FDM, differential quotients are introduced into the equation. After appropriate transformations, the Eq. (3) for the central nodes has the form:

$$T_{i,j}^f = T_{i,j}^{f-1} - \frac{\Delta t}{c_p \rho} \sum_{a=1}^{4} \frac{\Phi_e}{R_e} \left(T_e^{f-1} - T_{i,j}^{f-1} \right), \tag{13}$$

where $i = 2, 3, \ldots, n-1$, $j = 2, 3, \ldots, m-1$, n and m are the number of nodes in z- and r-direction, respectively; the individual a corresponds to $e = \{(i, j+1); (i, j-1); (i+1, j); (i-1, j)\}$. The shape function Φ_e and the thermal resistance R_e are defined as:

$$\Phi_{i,j-1} = \frac{r_{i,j} - 0.5h_1}{r_{i,j} h_1}, \quad \Phi_{i,j+1} = \frac{r_{i,j} + 0.5h_1}{r_{i,j} h_1}, \quad \Phi_{i-1,j} = \Phi_{i+1,j} = \frac{1}{h_2}, \tag{14}$$

$$R_{i,j-1} = R_{i,j+1} = \frac{h_1}{k}, \quad R_{i-1,j} = R_{i+1,j} = \frac{h_2}{k}, \tag{15}$$

where $r_{i,j}$ is the radial coordinate of the node (i, j); and h_1 and h_2 are the mesh steps in the r- and z-direction, respectively.

Similarly, for central nodes, Eq. (11) is of the form:

$$(c_d)_{i,j}^f = (c_d)_{i,j}^{f-1} - \Delta t \sum_{a=1}^{4} \frac{\Phi_e}{W_e} \left((c_d)_e^{f-1} - (c_d)_{i,j}^{f-1} \right), \tag{16}$$

where W_e is the mass resistance given by:

$$W_{i,j-1} = W_{i,j+1} = \frac{h_1}{D_{eff}}, \quad W_{i-1,j} = W_{i+1,j} = \frac{h_2}{D_{eff}}. \tag{17}$$

A detailed derivation of the Eq. (3) and for boundary nodes can be found, for example, in the thesis [5]. Eq. (6) needs to be completed with a stability condition:

$$\Delta t \leq \sum_{a=1}^{4} \frac{\Phi_e}{R_e} \quad and \quad \Delta t \leq \sum_{a=1}^{4} \frac{\Phi_e}{W_e}. \tag{18}$$

3. Results and discussion

The study analysed a homogeneous and porous material with the following properties. The thermophysical properties are equal to c_p = 3567.5 J·kg^{-1}·K^{-1}, ρ = 1100 kg·m^{-3} and k = 0.518 W·m^{-1}·K^{-1} [18], [19], while the porous properties are ε = 0.78 and τ = 1.4 [13]. The parameters used to calculate the diffusion coefficient were: r_s = 2.541×10^{-10} m, μ_d = 1.996×10^{-3} Pa·s, μ_d = 0.8905×10^{-3} Pa·s, $V_{c,d}$ = 228 mL·mol^{-1}, $V_{c,w}$ = 56 mL·mol^{-1} [13], [20], [21]. The initial values of temperature and concentration are equal to $T_{\text{init.}}$ = 22 °C, $c_{\text{init.}}$ = 0 %(w/w), while the natural convection heat transfer coefficient is α = 525 W·m^{-2}·K^{-1} [13]. The dimensions of the sample are R = 3 mm and H = 1 mm (cf. Fig. 1). The time and mesh steps are equal to: Δt = 0.005 s, h_1 = 0.1 mm and h_2 = 0.05 mm. The simulation stops after 100 s.

The computation were performed in an author's program prepared in MATLAB 2021a software, while UNIFAC model calculations were carried out using *UNIFAC group contribution method activity calculator function* (Saeed (2025); https://www.mathworks.com/matlabcentral/fileexchange/64885-unifac-group-contribution-method-activity-calculator-function, MATLAB Central File Exchange. Retrieved January 15, 2025).

Fig. 2 presents a graph of the temperature change over time as a result of alterations in the temperature of the bath solution, where the dashed line represents the change in T_{bath} in time. The results obtained are given for a point with coordinates (5×10^{-5}, 2.5×10^{-5}) m. Figure 3 illustrates the function of the effective diffusion coefficient in time assuming (a) the material is homogeneous and (b) the material is porous. One can see, a decrease in temperature also effects in a decrease in the diffusion coefficient value over time. It is also observed that the values of the diffusion coefficient for vary according to the model introduced. Higher values of this coefficient are observed for the porous material model.

The obtained effective diffusion coefficient values are worth comparing with data presented in the literature [13], [15]. For example, Yu et al. [13], [15] use a similar model for a porous material in their studies, except that it considers the dependence of the dynamic viscosity on the temperature. The values of the effective diffusion coefficient received by them for the porous material are lower than in this article.

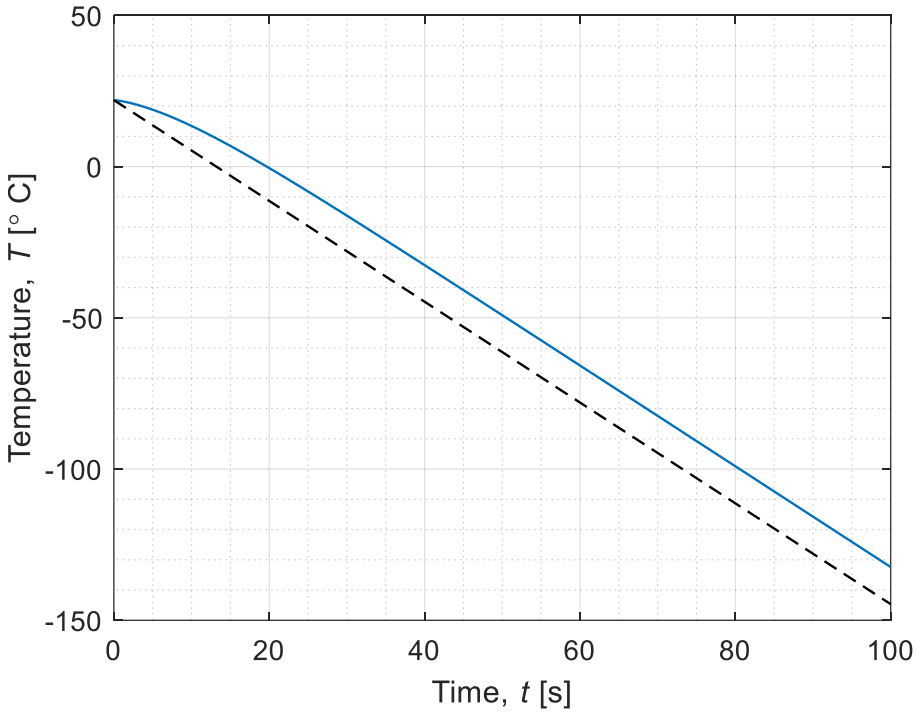

Fig. 2: Temperature as a function of time.

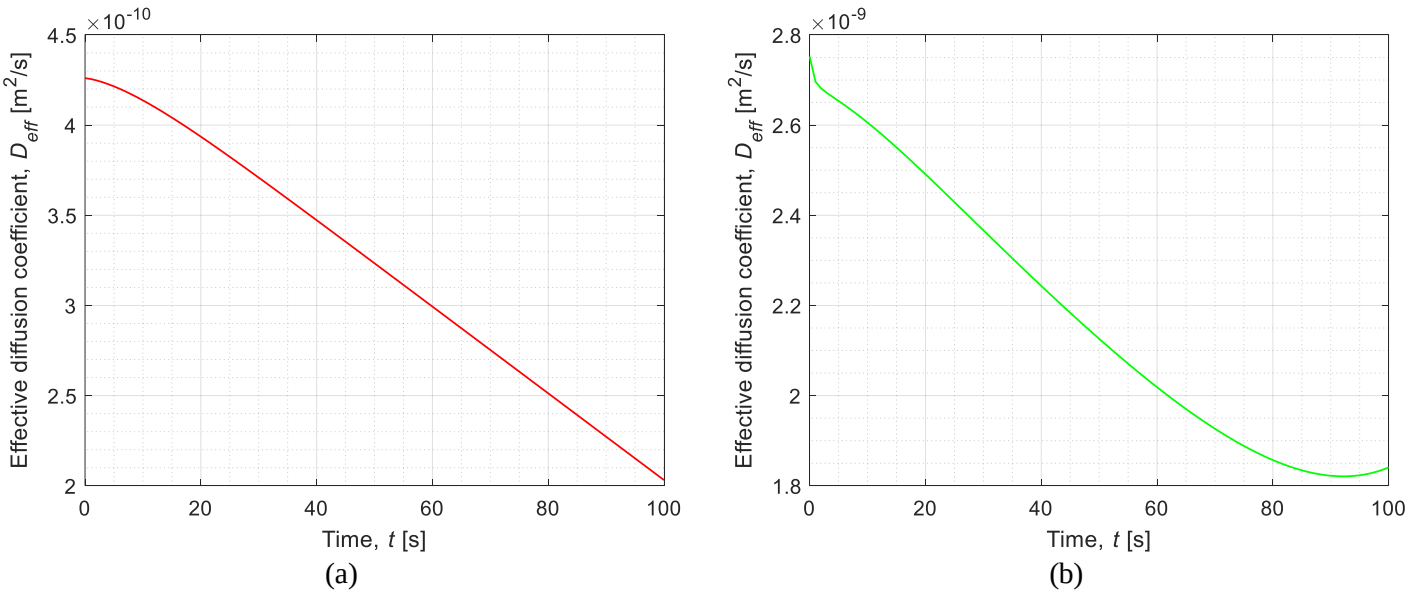

Fig. 3: Effective diffusion coefficient as a function of time for: (a) homogeneous material and (b) porous media.

4. Conclusion

The article presents a research on the diffusion coefficient for a selected biological tissue (an articular cartilage), which has been modelled as a homogeneous material and a porous material. The effective diffusion coefficient depends on the temperature distribution in the computational domain and, in the case of a porous medium model, also on the molar fraction changing due to the mass transfer phenomenon. The value of the effective diffusion coefficient decreases with a lowering of the temperature and is higher for a porous media than for a homogeneous material.

In conclusion, it can be deduced that the choice of an appropriate material model has a significant impact on the value of the effective diffusion coefficient. In further studies, it is planned to use an effective diffusion coefficient considering porosity to simulate the cryopreservation by slow freezing, vitrification or liquidus-tracking protocol. In this way, the model presented in this paper will be practically applicable to the analysis of real processes. On the other hand, it would be worth extending the model given by including the impact of temperature on dynamic viscosity (compare with [13], [15]).

Acknowledgements

Publication is funded by the Excellence Initiative – Research University programme realized at the Silesian University of Technology, in 2024-2026 (grant no. 10/040/SDU/10-22-03).

References

[1] K. Khanafer and K. Vafai, ‘A critical review on the applications of fluid-structure interaction in porous media’, *International Journal of Numerical Methods for Heat & Fluid Flow*, vol. 30, no. 1, pp. 308–327, 2020, doi: 10.1108/HFF-07-2019-0592.

[2] A.-R. A. Khaled and K. Vafai, ‘The role of porous media in modeling flow and heat transfer in biological tissues’, *International Journal of Heat and Mass Transfer*, vol. 46, no. 26, pp. 4989–5003, 2003, doi: 10.1016/S0017-9310(03)00301-6.

[3] A. Skorupa and A. Piasecka-Belkhayat, ‘Numerical Modeling of Heat and Mass Transfer during Cryopreservation Using Interval Analysis’, *Applied Sciences*, vol. 11, no. 1, p. 302, 2020, doi: 10.3390/app11010302.

[4] A. Piasecka-Belkhayat and A. Skorupa, 'Numerical Study of Heat and Mass Transfer during Cryopreservation Process with Application of Directed Interval Arithmetic', *Materials*, vol. 14, no. 11, p. 2966, 2021, doi: 10.3390/ma14112966.
[5] A. Skorupa, 'Multi-scale modelling of heat and mass transfer in tissues and cells during cryopreservation including interval methods', Doctoral thesis, Politechnika Śląska, Gliwice, Poland, 2023.
[6] A. Piasecka-Belkhayat, A. Skorupa, and M. Paruch, 'Determining Thermophysical Parameters of Cryopreserved Articular Cartilage Using Evolutionary Algorithms and Experimental Data', *Materials*, vol. 17, no. 23, 2024, doi: 10.3390/ma17235703.
[7] R. Behrou, H. Foroughi, and F. Haghpanah, 'Numerical study of temperature effects on the poro-viscoelastic behavior of articular cartilage', *Journal of the Mechanical Behavior of Biomedical Materials*, vol. 78, pp. 214–223, 2018, doi: 10.1016/j.jmbbm.2017.11.023.
[8] J. Ozwoniarek, H. Wiśniewska-Weinert, J. Lisowski, and Ł. Kędzia, 'Nowe rozwiązania w zakresie biotribologii i biomateriałów. Cz. 2 Stanowisko do badań zużyciowych elementów endoprotez stawu biodrowego', *Obróbka Plastyczna Metali*, vol. 18, no. 1, pp. 35–40, 2007 (in Polish).
[9] D. Majda, A. Bhattarai, J. Riikonen, B.D. Napruszewska, M. Zimowska, A. Michalik-Zym, J. Töyräs, V.-P. Lehto, 'New approach for determining cartilage pore size distribution: NaCl-thermoporometry', *Microporous and Mesoporous Materials*, vol. 241, pp. 238–245, 2017, doi: 10.1016/j.micromeso.2017.01.005.
[10] F. Xu, S. Moon, X. Zhang, L. Shao, Y. S. Song, and U. Demirci, 'Multi-scale heat and mass transfer modelling of cell and tissue cryopreservation', *Philosophical Transactions of the Royal Society A: Mathematical, Physical and Engineering Sciences*, vol. 368, no. 1912, pp. 561–583, 2010, doi: 10.1098/rsta.2009.0248.
[11] A. Skorupa and A. Piasecka-Belkhayat, 'Comparison of heat transfer phenomena for two different cryopreservation methods: slow freezing and vitrification', *Journal of Applied Mathematics and Computational Mechanics*, vol. 22, no. 1, pp. 53–65,. 2023, doi: 10.17512/jamcm.2023.1.05.
[12] W. Liu, G. Zhao, Z. Shu, T. Wang, K. Zhu, and D. Gao, 'High-precision approach based on microfluidic perfusion chamber for quantitative analysis of biophysical properties of cell membrane', *International Journal of Heat and Mass Transfer*, vol. 86, pp. 869–879, 2015, doi: 10.1016/j.ijheatmasstransfer.2015.03.038.
[13] X. Yu, S. Zhang, and G. Chen, 'Modeling the addition/removal of dimethyl sulfoxide into/from articular cartilage treated with the liquidus-tracking method', *International Journal of Heat and Mass Transfer*, vol. 141, pp. 719–730, 2019, doi: 10.1016/j.ijheatmasstransfer.2019.07.032.
[14] B. R. Bird, W. E. Stewart, and E. N. Lightfoot, *Transport Phenomena*, Drugie. United States of America: John Wiley & Sons, Inc, 2002.
[15] X. Yu, G. Chen, and S. Zhang, 'A Model to Predict the Permeation Kinetics of Dimethyl Sulfoxide in Articular Cartilage', *Biopreservation and Biobanking*, vol. 11, no. 1, pp. 51–56, 2013, doi: 10.1089/bio.2012.0050.
[16] A. Fredenslund, R. L. Jones, and J. M. Prausnitz, 'Group-contribution estimation of activity coefficients in nonideal liquid mixtures', *AIChE Journal*, vol. 21, no. 6, pp. 1086–1099, 1975, doi: 10.1002/aic.690210607.
[17] E. Majchrzak and B. Mochnacki, *Metody numeryczne: podstawy teoretyczne, aspekty praktyczne i algorytmy*, Wyd. 4 rozsz. i uzup.. Gliwice: Wyd. Politechniki Śląskiej, 2005 (in Polish).
[18] J.-I. Youn, S. A. Telenkov, E. Kim, N. C. Bhavaraju, B.J.F. Wong, J. W. Valvano, T. E. Milner, 'Optical and thermal properties of nasal septal cartilage', *Lasers in Surgery and Medicine*, vol. 27, no. 2, pp. 119–128, 2000, doi: 10.1002/1096-9101(2000)27:2<119::AID-LSM3>3.0.CO;2-V.
[19] Accessed: Jul. 10, 2024. [Online]. Available: https://itis.swiss/virtual-population/tissue-properties/database/
[20] Accessed: Jul. 10, 2024. [Online]. Available: https://www.trimen.pl/witek/ciecze/old_index.html (in Polish)
[21] B. M. Schulze, D. L. Watkins, J. Zhang, I. Ghiviriga, and R. K. Castellano, 'Estimating the shape and size of supramolecular assemblies by variable temperature diffusion ordered spectroscopy', *Org. Biomol. Chem.*, vol. 12, no. 40, pp. 7932–7936, 2014, doi: 10.1039/C4OB01373E.